Mapana – Journal of Sciences
2025, Vol. 24, No. 1, 1-22
ISSN 0975-3303 | https://doi.org/10.12723/mjs.72.1

Palmitic acid-induced endoplasmic reticulum stress links metabolic stress to senescence and regulates cell fate via PERK signalling in colon cancer cells

Valappan Veetil Soumya*, Snijesh Valiya Parambath†, Chevookaren Francis Binoy‡, Achuthan C Raghavamenon*, Suraj Kadunganattil* and Thekkekara Devassy Babu*

Abstract

Palmitic acid, a saturated fatty acid, promotes cancer progression and induces endoplasmic reticulum stress, which is associated with a misfolded/unfolded protein response. The study aims to explore the impact of metabolic stress induced by palmitic acid on cell fate decisions in colon cancer cell HCT15, with a specific focus on PERK signalling that connects metabolic stress to senescence. In the MTT assay, the $IC_{50\ was}$ determined to be 186 µM. The uptake of palmitic acid was confirmed by Oil Red O staining. Based on MTT and colony formation assays, the survival doses were identified as 50–100 µM, while lethal doses were determined to be 150–200 µM. Palmitic acid-induced oxidative stress is evidenced by increased ROS production, elevated MDA levels, and alterations in antioxidant activities. ER stress, driven by protein misfolding, was further confirmed through Thioflavin T staining. Gene expression analysis at survival doses revealed upregulation of ER stress and oxidative stress-related genes, including *Bip, CHOP, PERK, ATF4, Nrf2*, and *HO-1*, highlighting their role in promoting stress tolerance. Bioinformatics analysis of GEO datasets on senescence in HCT15 cells revealed a PERK-mediated pathway, supporting a link

* Department of Biochemistry, Amala Cancer Research Centre (Recognized Centre of University of Calicut), Thrissur - 680 555, Kerala, India, Email: soumyavvknr@gmail.com, raghav@amalaims.org, surajk@amalaims.org, babutharakan@gmail.com.

† Division of Molecular Medicine, St. John's Research Institute, Bangalore - 560 034 Karnataka, India. Email: snijesh@gmail.com.

‡ Research and Post-Graduate Department of Zoology, St. Thomas College (Autonomous), Thrissur – 680 001, Affiliated to University of Calicut, Kerala, India. Email: drcfbinoy@gmail.com.

between palmitic acid-induced metabolic stress and senescence. This study emphasises the critical role of palmitic acid-induced ER stress in connecting metabolic stress to senescence in colon cancer cells and the involvement of PERK signalling as a key mediator in this process. These insights provide a deeper understanding of how metabolic stress contributes to senescence, potentially revealing new therapeutic targets for managing colon cancer progression.

Keywords: Palmitic acid; ER stress; UPR; senescence; PERK pathway; colon cancer

1. Introduction

Palmitic acid, a saturated fatty acid prevalent in diets, has been linked to various cancers, influencing tumour growth and metastasis [1, 2]. This dietary component, commonly found in palm oil, dairy products, meats and processed food, has been reported to affect cellular functions by modulating lipid metabolism and promoting the development of a pro-tumorigenic microenvironment. Among its diverse biological effects, it was evident that palmitic acid induces endoplasmic reticulum (ER) stress by overwhelming the protein-folding machinery, thereby activating the unfolded protein response (UPR)[3]. Usually, the UPR is an adaptive mechanism designed to restore cellular balance; however, prolonged or dysregulated ER stress can significantly affect cell fate, potentially promoting either survival or cell death [4].

The UPR is a complex signalling network regulated by three key stress regulators, including protein kinase R-like ER kinase (PERK), activating transcription factor 4 (ATF4), and C/EBP homologous protein (CHOP) [5, 6]. These sensors regulate cell fate under ER stress by balancing protein-folding and cellular needs, promoting survival under mild stress, and initiating apoptosis under extreme stress [7, 8]. Among these, the PERK signalling axis is critical in modulating cell fate. Activation of PERK phosphorylates the eukaryotic initiation factor 2α (eIF2α), which reduces overall protein synthesis by selectively promoting the translation of activating transcription factor 4 (ATF4).ATF4, in turn, modulates genes involved in redox homeostasis, autophagy, and apoptosis, with downstream effectors such as C/EBP homologous protein (CHOP) playing pivotal roles in determining cell survival or death [5, 6].

In cancer, sustained ER stress often shifts the function of UPR from a transient adaptive response to a chronic survival mechanism, enabling tumour cells to endure unfavourable conditions such as nutrient deprivation, hypoxia, and therapeutic stress [9, 10]. Metabolic stress in cancer, caused by factors like nutrient deprivation and altered metabolism, exacerbates cellular

challenges [11, 12]. This disrupts homeostasis and triggers a maladaptive shift in the UPR, leading to chronic activation of UPR pathways due to misfolded protein accumulation. The interplay between metabolic and ER stress creates a cycle that promotes tumour cell survival and adaptability, enhancing resistance to therapeutic interventions[13, 14]. Palmitic acid-induced metabolic stress adds another layer of complexity to ER stress in cancer. By altering lipid composition and disrupting ER membrane integrity, palmitic acid exacerbates protein misfolding and oxidative stress, leading to heightened ER stress. Oxidative stress, driven by excessive reactive oxygen species (ROS) production, was found to synergise with ER stress in promoting cancer cell survival and resistance to apoptosis [2]. Furthermore, the interplay between oxidative stress and UPR pathways enhances tumour cell adaptability, contributing to chemoresistance and disease progression [3].

Senescence, characterised by irreversible cell cycle arrest, is a crucial cellular response to various stressors. [15] Recent evidence indicates that ER stress, mediated through the PERK signalling pathway, significantly drives senescence under stress conditions.[16, 17]. Despite growing insights into ER stress in cancer, the role of palmitic acid-induced metabolic stress in colon cancer cell survival and its link to senescence remains unexplored. Furthermore, colon cancer is the most prevalent malignancy worldwide, with its progression significantly influenced by metabolic and inflammatory factors[18, 19]. This study investigates the effects of palmitic acid-induced metabolic and ER stress on HCT15 colon cancer cells, focusing on how UPR signalling modulates cell survival under these conditions. Through bioinformatics analysis of relevant GEO datasets examining factors such as hypoxia and glucose deprivation in HCT15 cells, this research delves into the contribution of ER stress to cellular senescence. The findings highlight a critical connection between the PERK/ATF4 pathway and senescence, emphasising its central role in metabolic stress responses and colorectal cancer progression. These insights pave the way for identifying novel therapeutic targets to overcome treatment resistance and curb cancer progression.

2. Materials and methods

2.1. Cell culture and treatment

HCT15 colon cancer cells, obtained from NCCS, were maintained in RPMI-1640 medium supplemented with FBS (10%) and penicillin/streptomycin (1%) under controlled conditions of 37°C and 5% CO_2. Cells were treated for 24 hours with palmitic acid (100 mM in ethanol stock), ensuring the final vehicle concentration in the culture medium remained below 0.2%.

2.2 Cytotoxicity and viability assays

Cell viability in HCT15 cells was assessed using the MTT assay and trypan blue exclusion [20, 21]. For the MTT assay, cells (5×10^3/well) were treated with increasing palmitic acid concentrations for 24 hrs, followed by MTT addition (5 mg/mL, 20 µL/well) and 4-hr incubation. Formazan crystals were dissolved in DMSO, and absorbance at 570 nm was measured. The viability of cells after palmitic acid treatment was confirmed using trypan blue exclusion by counting viable and dead cells with a hemacytometer at 50-200 µm.

2.3. Lipid uptake analysis by Oil Red O staining

Neutral lipid accumulation was assessed using the Oil Red O staining method [22]. Post palmitic acid treatment, cells were washed with PBS, fixed with 4% formaldehyde, and stained with Oil Red O for 30 minutes. The stained cells were imaged, and lipid content was quantified by extracting the dye with isopropanol and measuring absorbance at 510 nm using a microplate reader.

2.4. Colony formation assay

Treated cells were PBS-washed, trypsinised, and reseeded at 3,000 cells per well in duplicate 6-well plates. After 15 days of incubation at 37°C, colonies were fixed with methanol and stained with 0.5% crystal violet. Images were captured using a phase-contrast microscope, colonies were counted, and the surviving fractions were calculated [23].

2.5. Reactive oxygen species (ROS) analysis

Treated cells were incubated with 10 µM DCFH-DA (2′,7′-dichlorodihydrofluorescein diacetate) for 30 minutes at 37°C. DCFH-DA was deacetylated intracellularly to DCFH, which ROS oxidised to form the fluorescent DCF. Fluorescence intensity was measured using a BioTek plate reader (excitation: 485 nm; emission: 530 nm). H2O2 (100µM) was treated as positive control 6 hrs before reading. ROS generation was quantified from normalised fluorescence intensity [24].

2.6. Analysis of antioxidant status and lipid peroxidation

Cell lysates were prepared, and total protein content was quantified [25]. Antioxidants, including catalase (CAT)[26], superoxide dismutase (SOD) [27], glutathione S-transferase (GST) [28, 29], glutathione reductase (GR) [30, 31], reduced glutathione (GSH)[32], and glutathione peroxidase (GPx) [33], were measured as described in the respective references. Lipid peroxidation was assessed by determining malondialdehyde (MDA) level using the TBARS method [34].

2.7. Thioflavin T staining for misfolded protein aggregation

Thioflavin T (ThT) staining was performed to visualise misfolded protein aggregates indicative of ER stress. Treated cells were fixed with 4% paraformaldehyde. After washing, cells were incubated with 0.01% ThT for 30 minutes in the dark. The cells were rewashed and imaged using a fluorescence microscope with excitation at 450 nm and emission at 482 nm. ThT fluorescence intensity was quantified using spectrofluorimetric analysis. Tunicamycin (3 µM) was used as a positive control and applied 6 hours before the reading [35].

2.8. Gene expression analysis by RT-*q*PCR

For gene expression analysis, cells treated with 50 µM and 100 µM palmitic acid were harvested for total RNA extraction using the RNeasy Mini Kit (Qiagen) following the manufacturer's protocol. RNA concentrations and purity were determined by spectrophotometry (Nanodrop 2000). Reverse transcription was performed using the Superscript IV Reverse Transcriptase, and RT-PCR was carried out with specific primers for genes involved in ER stress (BIP, CHOP, PERK, ATF4, IRE1, XBP1), oxidative stress (NQO1, HO-1, NRF2), and drug resistance markers. The reaction was performed on a Step OnePlus™ Real-Time PCR System. Relative Gene expression was measured using the $2^{-\Delta\Delta Ct}$ method, normalised to GAPDH [36].

Table 1: Human primer sequences used in the study were as follows:

Gene	Forwarded primer	Reverse primer	Product size
PERK	5'ATTGCATCTGCCTGGTTAC3'	5'GACTCCTTCCTTTGCCTGT3'	650
ATF4	5'CCAGCAAAGCACCGCAACA3'	5'CCATCCACAGCCAGCCATT3'	215
NRF2	5'AGACAAACATTCAAGCCGCT3'	5'CCATCTCTTGTTTGCTGCAG3'	438
NQO1	5'AAGGATGGAAGAAACGCCTGGAGA3'	5'GGCCCACAGAAAGGCCAAATTTCT3'	156
HO1	5'ACGCGTTGTAATTAAGCCTCGCAC3'	5'TTCCGCTGGTCATTAAGGCTGAGT3'	176
ATF6	5'CAGGGAGAAGGAACTTGTGA3'	5' ACTGACCGAGGAGACGAGA3'	344
CHOP	5'AAGGCACTGAGCGTATCATGT3'	5'TGAAGATACACTTCCTTCTTGAACA3'	105
GAPDH	5'GACATGCCGCCTGGAGAAAC3'	5'AGCCCAGGATGCCCTTTAGT3'	92

2.9. Analysis of GEO data from HCT15 colon cancer cells under ER Stress conditions

Gene expression data for HCT15 colon cancer cells under ER stress conditions (GSE227379) were analysed [37]. The dataset, generated on the Illumina NovaSeq 6000 platform, included nine samples: three biological replicates each for control, hypoxia ($CoCl_2$ treatment), and low-glucose conditions. Differential expression analyses compared hypoxia vs. control and low-glucose vs. control groups. Raw FASTQ files underwent quality control with FastQC, and low-quality reads, and adaptor sequences were removed using Trim Galore [38, 39]. High-quality reads were aligned to the GRCh38

reference genome using STAR**,** followed by gene quantification with feature counts [40, 41].

Differential expression analysis was performed with DESeq2, which accounts for biological variability and library size differences [42, 43]. Genes with a fold change ≥1.5 and adjusted p-value <0.05 were identified as significantly differentially expressed. Common DEGs between hypoxia and low-glucose conditions were determined using a Venn diagram. KEGG signalling pathway analysis using ShinyGO 0.82 identified significantly enriched pathways (FDR < 0.05), excluding genes without KEGG annotations. Functional analysis of the shared DEGs was conducted using ShinyGO for pathway enrichment, and a network visualisation of gene-pathway interactions was created in Cytoscape. (Shinygo: http://bioinformatics.sdstate.edu/go77/)

2.10. Statistical analysis

The data analysis utilised Mean ± SEM (Standard Error of the Mean) with GraphPad Prism. For three independent in vitro experiments, one-way ANOVA was conducted for multiple comparisons, followed by Tukey's post-hoc test. Statistically significant results were indicated by p-values of * < *0.05,* ** < *0.01,* and *** < *0.001.*

3. Results

3.1 Impact of palmitic acid on cell viability, neutral lipid accumulation, and colony formation in HCT15 colon cancer cells

The toxicity of palmitic acid was initially evaluated in HCT15 colon cancer cells using the MTT assay, which revealed a dose-dependent effect with an IC50 of 186 µM (Fig. 1A). Based on this IC_{50} value, doses of 50, 100, 150, and 200 µM were selected for further analysis. The trypan blue assay confirmed dose-dependent cell viability with the following results: 79.63 ± 0.52%, 68.72 ± 1.45%, 57.87 ± 1.01%, and 47.24 ± 1.7% at 50, 100, 150, and 200 µM, respectively (Fig. 1B). Palmitic acid uptake was measured using Oil Red O staining, which proved the accumulation of neutral lipids in cells at the specified concentrations (Fig.1C). Spectrophotometric analysis of lipid uptake revealed a progressive increase in intracellular lipid content up to 150 µM, with relative values of 2.02 ± 0.31, 2.53 ± 0.51, and 2.80 ± 0.38, respectively. However, at 200 µM, lipid accumulation decreased to 2.23 ± 0.29, suggesting significant toxicity at this concentration (Fig. 1D).

A colony formation assay was performed to evaluate cell survival doses further. Results showed that the cells formed healthy colonies at 50 and 100 µM palmitic acid after treatment, while colony formation was significantly reduced at 150 and 200 µM (Figure 1E). The survival fractions were 0.88 ± 0.02, 0.79 ± 0.19, 0.05 ± 0.009, and 0.005 ± 0.001 for 50, 100, 150, and 200 µM, respectively (Fig. 1F), indicating a sharp decline in survival at 150 and 200 µM.

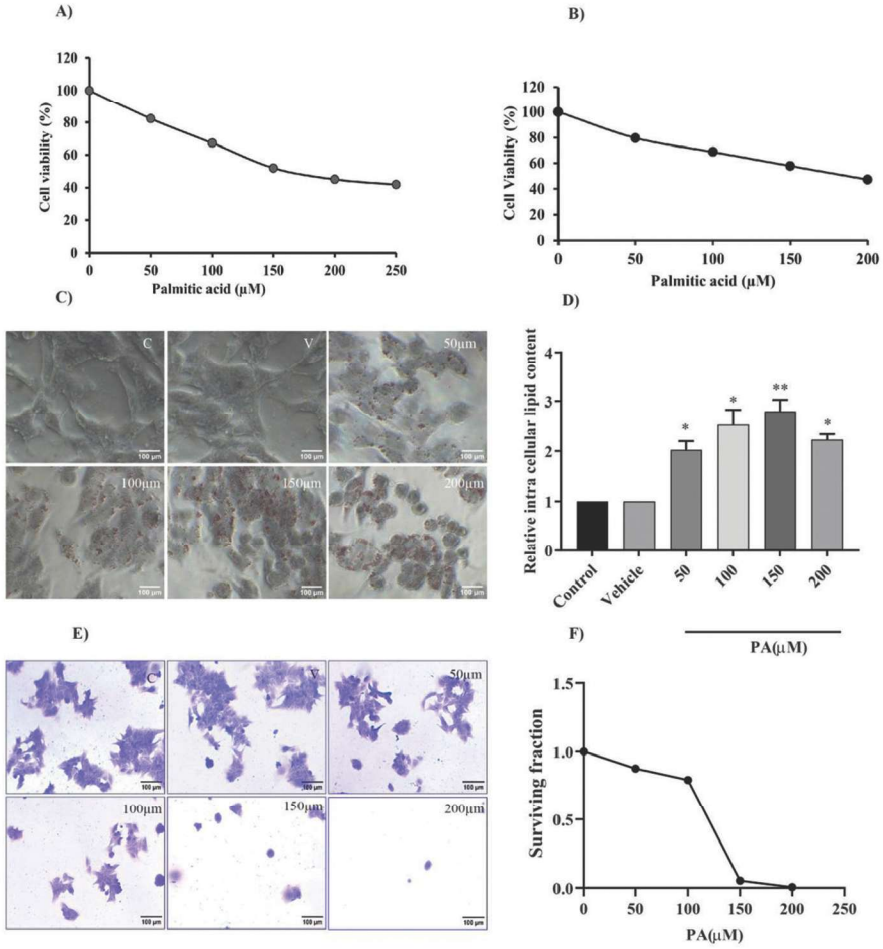

Figure 1: Effects of PA on viability, lipid accumulation, and colony formation in HCT15 cells. HCT15 cells treated with varying PA concentrations of 50,100,150 and 200 were assessed for cytotoxicity by MTT assay (A) and viability by Trypan blue exclusion (B). Lipid accumulation was evaluated through Oil Red O staining with phase-contrast microscopy (magnification 400x, scale bar 100um) (C) and quantified as relative intracellular lipid content (D). Colony formation was examined via crystal violet staining (E), and the survival fraction was calculated relative to controls (F). Statistical significance was assessed using one-way ANOVA and Tukey's post-hoc test, with significance levels indicated as $^{**}P < 0.01$, $^{*}P < 0.05$.

3.2 Palmitic acid triggers oxidative stress in colon cancer cells

The exposure of HCT15 cells to palmitic acid resulted in a marked elevation of ROS levels, as indicated by a dose-dependent increase in the green fluorescence intensity of DCFH-DA (Fig.2A). Spectrofluorimetric analysis of palmitic acid-treated cells revealed the following relative fold changes in fluorescence intensity: 1.92 ± 0.15, 2.21 ± 0.21, 2.35 ± 0.29, and 1.94 ± 0.32 at palmitic acid concentrations of 50, 100, 150, and 200 µM, respectively. The reduction in fluorescence intensity at 200 µM is likely attributed to reduced cell viability due to the extreme toxicity of palmitic acid (Fig.2B).

Further analysis of antioxidant levels demonstrated an increase in SOD and CAT at 50 and 100 µM palmitic acid, followed by a decline at 150 µM. Glutathione-related antioxidants, including GST, GR, GPx, and GSH, remained stable up to 100 µM but decreased significantly at 150 µM. The MDA level, a lipid peroxidation marker, remained stable up to 100 µM but increased substantially at 150 µM (Fig. 2C & Table 2).

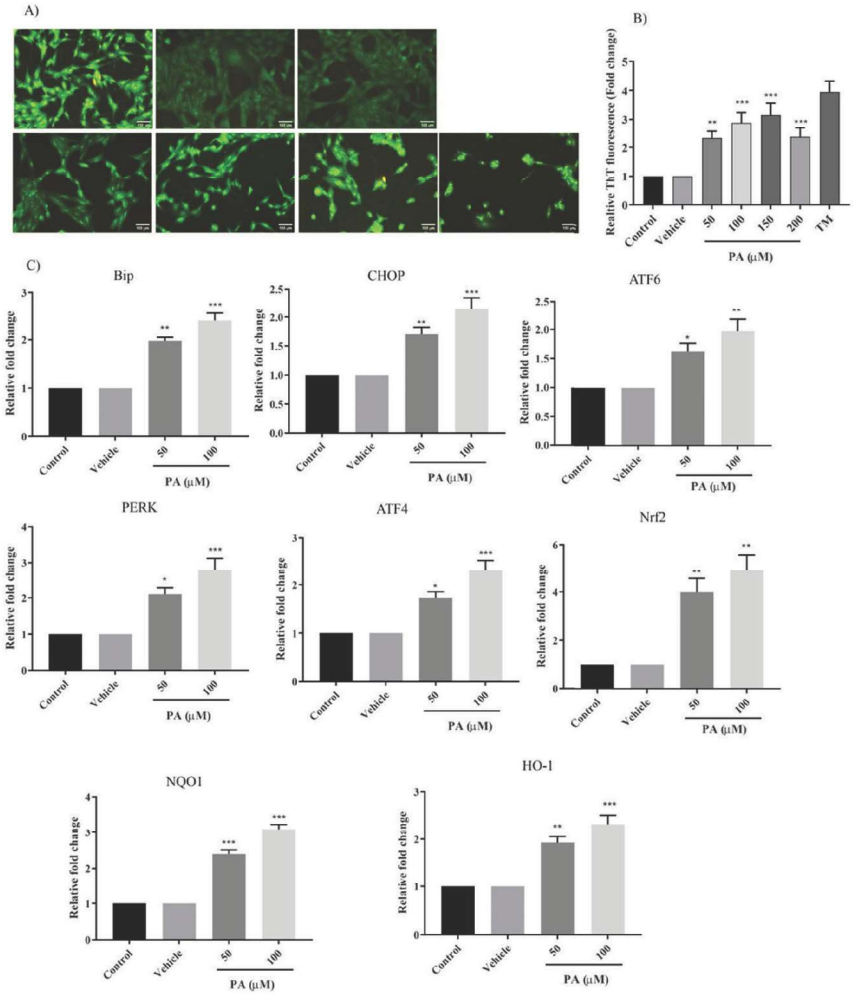

Figure 2: Palmitic acid-induced oxidative stress in colon cancer cells. HCT15 cells treated with PA were subjected to oxidative stress analysis. **(A)** Fluorescent microscopic images of DCFH-DA staining for ROS detection, captured at 400× magnification (scale bar: 100 µm). **(B)** Quantitative spectrofluorimetric analysis of relative DCF fluorescence expressed as relative fold change. **(C)** Graphical representation of the levels of different antioxidants and MDA following PA treatment. Data are presented as mean ± SEM, with statistical significance indicated by ***$p < 0.001$, *$p < 0.05$ and **$p < 0.01$.

Table 2: Elevated antioxidant levels and MDA in palmitic acid-treated HCT15 cell lysates:

Enzymes	Control	Vehicle	50μm	100μm	150μm	200μm
SOD	15.23±2.97	16.12±3.07	27.53±3.59*	35.9±4.02***	41.23±4.62***	24.38±3.71
CAT	9.26±0.93	9.18±1.11	16.91±1.99**	19.17±2.37**	22.86 ±3.2***	10.60±2.48
GST	3.24± 0.31	3.36±0.35	3.412±0.21	3.324±0.34	2.34±0.23*	2.19±0.239**
GR	4.24±0.52	4.39±0.416	4.647±0.52	4.72±0.39	3.02±0.31*	2.36±0.34**
GPX	15.2±2.14	15.02±2.37	14.09±2.38	13.72±2.13	8.56±2.16*	3.41±0.52
GSH	15.23±2.5	15.41±2.42	14.92±3.33	14.80±3.46	12.9±2.74*	7.49±2.95**
MDA	115.33±9.8	114.27±7.99	126.36±11.75	130.26±10.88	161.17±12.05**	91.33±10.3

3.3 Palmitic acid-induced metabolic stress in HCT15 colon cancer cells

Palmitic acid-induced metabolic stress in HCT15 colon cancer cells across all tested concentrations (50, 100, 150, and 200 µM), as evidenced by increased lipid accumulation, elevated reactive oxygen species (ROS) production, and altered antioxidant levels. At 50 and 100 µM, cells demonstrated tolerance to the induced stress, characterised by upregulated antioxidant responses. However, exposure to 150 and 200 µM palmitic acid led to significant cytotoxicity, as reflected by a reduced colony-forming ability. These findings demonstrate the dose-dependent nature of palmitic acid-induced metabolic stress, where lower concentrations promote tolerance while higher concentrations induce cytotoxicity.

3.4 Influence of palmitic acid on ER stress and PERK/ATF4 Signalling in regulating antioxidant responses

The influence of palmitic acid on ER stress and PERK/ATF4 signalling in regulating antioxidant responses was investigated in HCT15 cells. Increased misfolded protein aggregates in palmitic acid-treated HCT15 cells were indicated by enhanced green fluorescence from Thioflavin T staining, reflecting elevated ER stress (Fig.3A). Quantitative analysis revealed relative fluorescence intensities of 2.33 ± 0.24, 2.87 ± 0.37, 3.15 ± 0.41, and 2.36 ± 0.31 for palmitic acid concentrations of 50, 100, 150, and 200 µM, respectively, with the positive control (Tunicamycin™) showing intensity of 3.95 ± 0.37. A dose-dependent increase in misfolded protein aggregates was observed up to 150 µM palmitic acid, with a decline in intensity at 200 µM due to extreme toxicity and cell loss (Fig.3A).

The levels of ER stress markers were measured for survival doses of palmitic acid at 50 and 100 µM. BIP expression exhibited fold changes of 1.98 ± 0.12 and 2.4 ± 0.27 at these doses. CHOP expression levels were 1.71 ± 0.20 and 2.16 ± 0.33, while ATF6 expression levels were 1.63 ± 0.23 and 1.98 ± 0.36. PERK expression levels were 2.1 ± 0.31 and 2.8 ± 0.57, and ATF4

expression levels were 1.73 ± 0.22 and 2.31 ± 0.37 for the 50 and 100 µM treatments, respectively. The antioxidant genes Nrf2, NQO1, and HO-1 were upregulated in response to palmitic acid. Nrf2 expression was 4.01 ± 0.98 and 4.93 ± 1.17, NQO1 expression was 2.40 ± 0.19 and 3.10 ± 0.23, and HO-1 expression was 1.93 ± 0.21 and 2.33 ± 0.32 at the two concentrations, respectively (Fig. 3C).

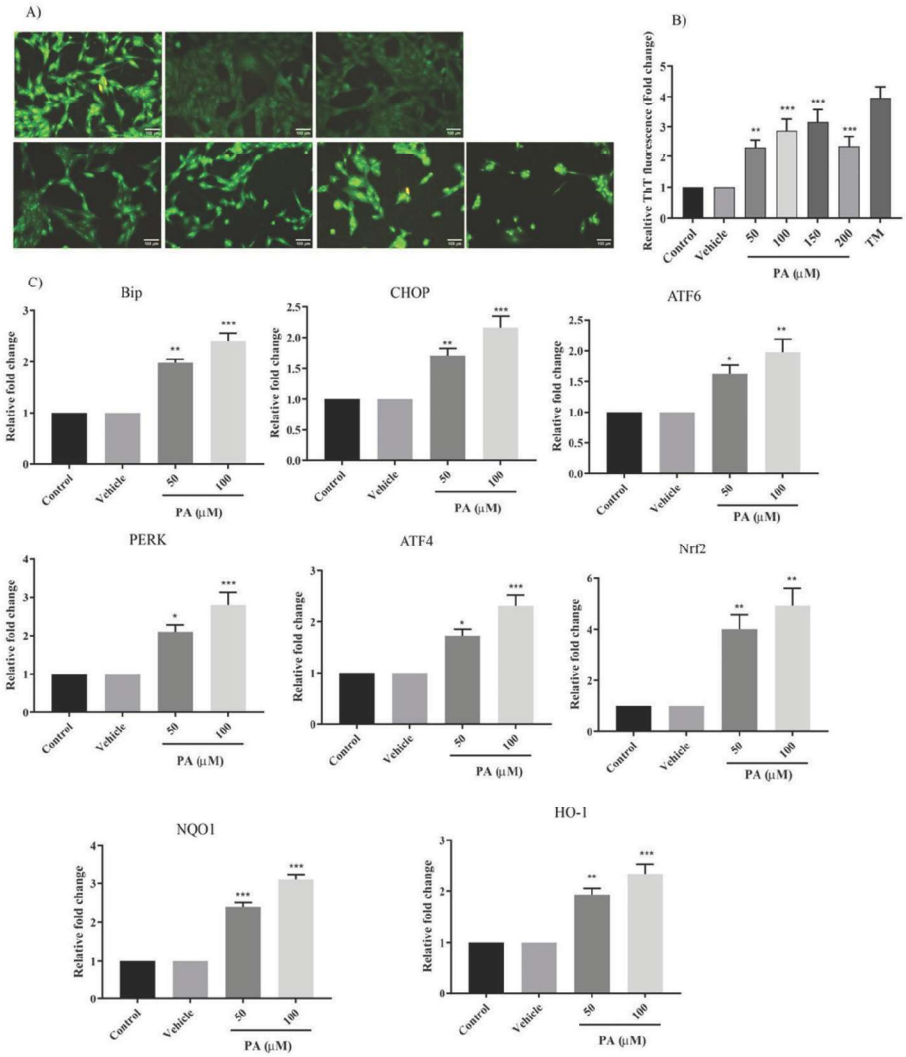

Figure 3: Development of ER stress in HCT15 cells upon PA treatment. HCT15 cells were treated with palmitic acid to assess ER stress markers. **(A)** Fluorescent microscopic images of ThT staining, visualising misfolded protein aggregation, captured at 400× magnification (scale bar: 100 µm). **(B)** Quantification of misfolded protein aggregation in cells represented as relative fold change. **(C)** RT-PCR analysis showing the relative fold change in the expression of ER stress, UPR, and antioxidant genes (BIP, CHOP, ATF6, PERK, ATF4) in response to PA treatment at 50 and 100 µM concentrations. Data are presented as mean ± SE, with statistical significance denoted by ***$p < 0.001$, *$p < 0.05$ and **$p < 0.01$.

3.5. Identification of shared upregulated genes in response to hypoxia and nutrient deprivation in HCT-15 colon cancer cells

Boxplot analysis of normalised gene expression data under hypoxia and nutrient deprivation conditions demonstrated consistent median values and no significant outliers. The uniform distribution of gene expression values across biological replicates, as well as their clustering in PCA plots, further validated the dataset's reliability for differential expression analysis (*Suppl. Fig. 1& Fig. 4A*). Differential expression (DEG) analysis identified 1,073 and 3733 genes as significantly upregulated under hypoxia and nutrient deprivation conditions, respectively. Among these, 1,034 genes were commonly upregulated under both conditions, suggesting shared transcriptional responses to these ER stress conditions (Fig. 4B & C).

3.6. PERK-mediated stress response and negative regulation resulting in senescence in HCT15 cells

Gene ontology analysis of commonly upregulated genes under hypoxia and nutrient deprivation revealed the activation of the PERK-mediated UPR, pathways of negative regulation, and signal transduction by the p53 class, all associated with senescence-induced cell cycle arrest. Specifically, the PERK-mediated unfolded protein response, under ER stress conditions, influences negative regulation and p53 pathways, which are critical in various cellular processes to overcome unfavourable conditions, indicating stress tolerance[17, 44, 45]. In addition, apoptotic pathways are also activated, suggesting severe ER stress in some cells. This observation highlights the heterogeneity of cancer cells, as some exhibit stress tolerance while others undergo cell death, as seen in HCT15 colon cancer cells (Fig. 4D).

Enrichment and network analyses revealed seven significantly enriched pathways (adjusted p-value < 0.05), three directly relevant to the study. The p53 signalling pathway (FDR = 1.2E-04, Fold Enrichment = 5.3) and transcriptional misregulation in cancer (FDR = 6.9E-03, Fold Enrichment = 2.7) were prominently enriched, highlighting their roles in regulating cell cycle arrest and senescence. Key p53 pathway genes, including *CDKN1A (p21)*, *GADD45A*, *BBC3*, and *SESN1*, were upregulated under stress, driving HCT15 cells into senescence by halting proliferation to prevent damage. *CDKN1A* mediated cell cycle arrest, *GADD45A* facilitated DNA repair, while *BBC3* and *SESN1* promoted stress-induced senescence. The transcriptional misregulation in cancer pathways involving *CDKN1A*, *GADD45A*, *MDM2*, and *CCND2* highlighted the contribution of dysregulated transcriptional pathways, notably p53, to senescence. Enrichment of the ferroptosis pathway (FDR = 1.2E-04, Fold Enrichment = 7.3) indicated oxidative stress-induced cell death driven by lipid peroxide accumulation, with severe ER stress triggering cell death in some cells. Significant pathways, including one-carbon folate,

ribosome, and COVID-19, were not central to the study's objectives (Fig. 4E, F). Analysis of the KEGG p53 signalling pathway (hsa04115) revealed that hypoxia and nutrient deprivation activate p53 signalling, upregulating effectors such as *p21* and *GADD45*, inducing cell cycle arrest and senescence under ER stress in HCT15 colon cancer cells (Fig. 5).

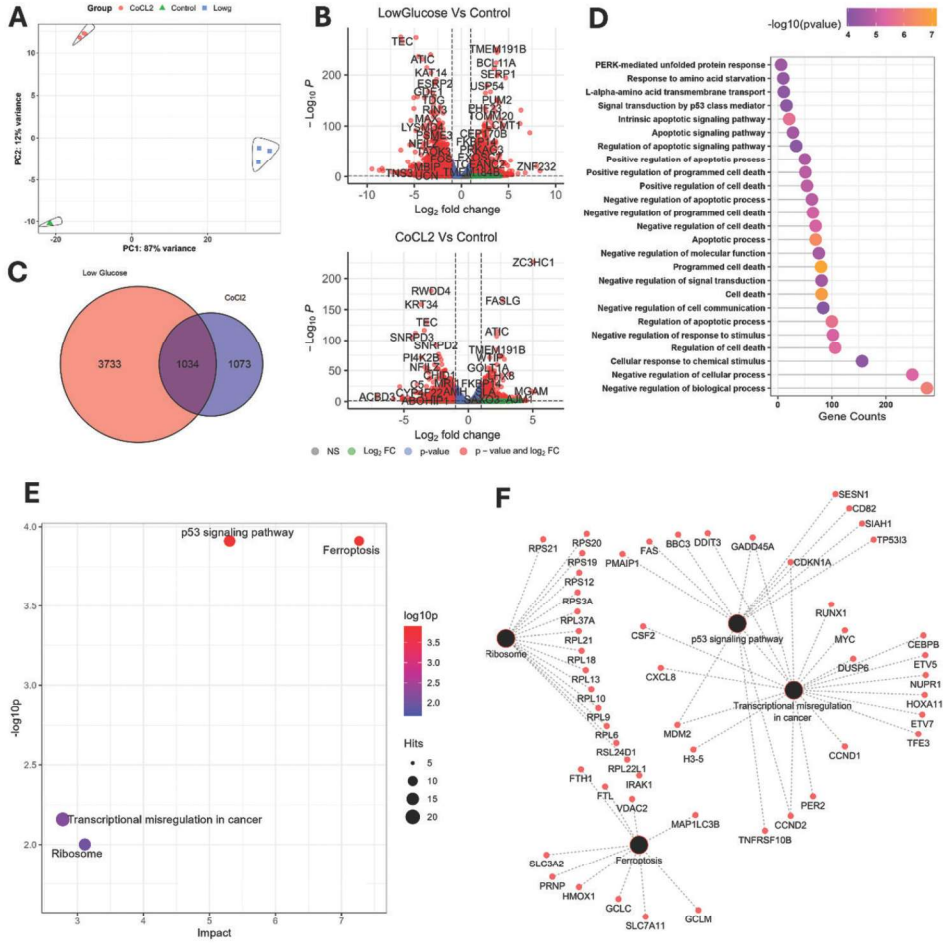

Figure 4: GEO data analysis of two ER stress conditions: hypoxia ($CoCl_2$) and nutrient deprivation (low glucose) in HCT15 colon cancer cells.

Gene expression data from GEO were analysed to assess the impact of hypoxia ($CoCl_2$) and nutrient deprivation (low glucose) on ER stress in HCT15 cells. **(A)** PCA analysis of gene expression in response to hypoxia and nutrient deprivation. **(B)** Volcano plot illustrating differentially expressed genes under hypoxic ($CoCl_2$) and nutrient-deprived (low glucose) conditions. **(C)** Venn diagram showing common DEGs identified in both hypoxia and nutrient deprivation conditions. **(D)** Dot plot displaying the biological processes associated with differentially expressed genes. **(E)** Fold Enrichment analysis highlighting significantly enriched pathways **(F)** Network analysis of genes from enriched pathways.

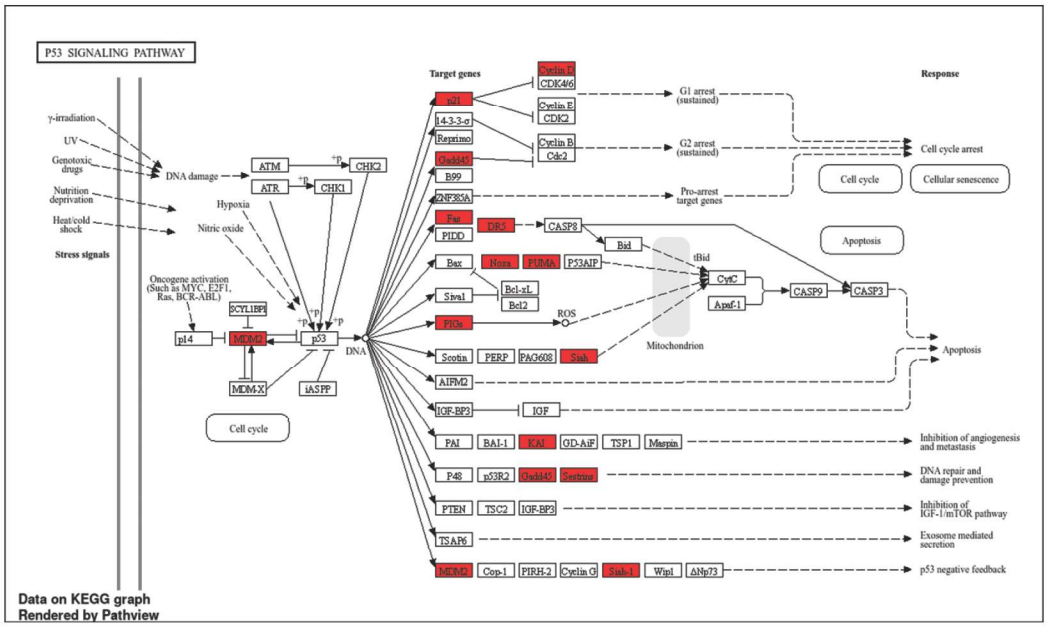

Figure 5: KEGG pathway analysis of common genes from hypoxia and nutrient deprivation. The KEGG analysis identified the *p53 signalling pathway* (hsa04115) as significantly enriched among the common differentially expressed genes under hypoxic ($CoCl_2$) and nutrient-deprived (low glucose) conditions.

4. Discussion

Palmitic acid significantly influences various cellular processes, including metabolism, oxidative stress, and protein homeostasis [46, 47]. In cancer cells, palmitic acid-induced metabolic reprogramming supports rapid growth and tumour progression, with ER stress playing a pivotal role in adapting to these metabolic challenges [48-50]. The current study examined the impact of palmitic acid on metabolic and ER stress in HCT15 colon cancer cells, focusing on the interplay between lipid accumulation, antioxidant responses, and the UPR. The study specifically examined how palmitic acid-induced metabolic stress activates the PERK arm of the UPR, linking lipid overload and metabolic stress to cellular senescence. The findings highlight the critical role of PERK signalling in coordinating cellular adaptation to PA-induced metabolic stress, driving senescence under moderate stress conditions while triggering cell death under extreme stress. Studying senescence, characterised by a permanent or premature exit from the cell cycle, is crucial as it allows cancer cells to adapt to stress, survive adverse conditions, and contribute to drug resistance[51, 52]. Understanding these mechanisms is vital for developing strategies to overcome therapeutic resistance and enhance treatment outcomes.

Our findings demonstrate that palmitic acid induces dose-dependent responses in HCT15 cells, promoting survival at lower concentrations (50 and

100 µM) and cytotoxicity at higher doses (150 and 200 µM). PA triggered lipid accumulation and increased ROS levels at all doses, indicating metabolic and oxidative stress [53-55]. A post-treatment colony formation assay revealed that lower concentrations supported colony formation while higher doses inhibited it. At "survival doses" (50 and 100 µM), adaptive mechanisms such as increased antioxidant enzyme activity (SOD and catalase) and lipid droplet formation mitigated ROS-induced damage. The lack of significant changes in glutathione-related antioxidants suggests the cell manages oxidative stress without depleting glutathione reserves. At "lethal doses" (150 and 200 µM), ROS accumulation overwhelmed antioxidant defences, leading to lipid peroxidation, glutathione depletion (measured by MDA), cellular damage, and reduced viability. The accumulation of oxidative stress surpasses compensatory mechanisms and may trigger apoptosis or necrosis[56, 57]. These dose-dependent effects highlight the balance between adaptive responses and oxidative damage, where excessive stress can overwhelm the cell's capacity to maintain homeostasis, leading to cell death, consistent with prior studies on metabolic stress [58-60].

As palmitic acid induces oxidative and metabolic stress, it contributes to toxicity in cancer cells while simultaneously promoting tumour progression and metastasis [2, 61-64]. This dual effect raises important questions about how palmitic acid can both promote cell death and facilitate cancer progression, highlighting the need for further investigation into the underlying mechanisms. In this context, ER stress, a key oxidative or metabolic stress consequence, is critical in cellular responses, influencing survival or apoptosis through the UPR. It also facilitates tumour initiation, progression, and metastasis by enabling cancer cells to adapt to adverse conditions. Moreover, UPR pathways such as IRE1/XBP1, PERK/ATF4, and ATF6 regulate survival, proliferation, and migration [9, 65]. Activation of the UPR, particularly the PERK pathway, has been identified in response to palmitic acid-induced stress [66, 67]. The PERK arm is crucial for cancer-related cellular stress, supporting proliferation progression [68, 69]. Consistent with previous findings, the current study also identified misfolded protein aggregates at survival doses, confirming palmitic acid-induced ER stress. The stress is accompanied by the upregulation of ER stress and UPR markers, such as BIP, CHOP, PERK, ATF4, and ATF6, and the activation of the PERK pathway, which promotes stress adaptation by reducing protein synthesis and enhancing protein folding [7, 70].

The study focused on adaptive responses, so RT-*q*PCR was not performed due to extreme toxicity and limited cell availability at lethal doses. CHOP expression was dose-dependent at survival doses, where adaptive responses predominated, though some cells still underwent death, as indicated by low CHOP levels. These findings are consistent with previous research showing that prolonged stress overwhelms PERK-mediated protective mechanisms,

leading to chronic ER stress and the upregulation of CHOP-induced pro-apoptotic factors. [71, 72]. This shift from adaptation to toxicity drives cell death, highlighting the dual role of the UPR in promoting survival under moderate stress and apoptosis under excessive stress [3, 73]. In line with previous studies, our study reported that the PERK/ATF4 pathway upregulated antioxidant genes (NRF2, NQO1, HO-1), essential for cellular homeostasis under oxidative stress [74-77].

One ER stress survival pathway involves tissue-specific UPR activation, leading to senescence in cancer cells, which can result from drug resistance or stressors independent of drug influx[55, 78, 79]. The PERK/ATF4 axis induces senescence under various stress conditions in cancer cells [17, 80]. GEO analysis of common genes under two ER stress conditions—$CoCl_2$-induced hypoxia and low-glucose-induced glucose deprivation—in HCT15 colon cancer cells demonstrated PERK-mediated activation of unfolded protein responses, negative regulation of cellular processes, p53 signalling, and apoptosis, as identified through Gene Ontology analysis. This negative regulatory mechanism suggests a slowdown in cellular processes and cell cycle arrest, consistent with previous research linking PERK-mediated unfolded protein responses to the p53 signalling pathway, contributing to senescence [44, 81, 82].

The study highlights the role of the p53 signalling pathway and transcriptional misregulation in cancer during ER stress in HCT15 cells. KEGG analysis indicates that the activation of p53 leads to cell cycle arrest and senescence, supported by the upregulation of key genes like p21 and GADD45 [83, 84]. Transcriptional misregulation involving CDKN1A, GADD45A, MDM2, and CCND2 further promotes senescence through dysregulated p53 pathways[85]. The ferroptosis pathway, linked to oxidative stress, involves SESN1 and BBC3, driving stress-induced senescence and cell death [86, 87]. This dual response reflects population heterogeneity, with stress-tolerant cells entering senescence and stress-intolerant cells dying. Overall, the findings confirm that ER stress activates PERK-mediated unfolded protein responses leading to senescence, with palmitic acid-induced metabolic stress also triggering PERK responses and linking metabolic stress to senescence in HCT15 cells.

5. Conclusion

Palmitic acid-induced ER stress in HCT15 colon cancer cells is mediated through the PERK-mediated pathway, establishing a connection between metabolic stress, cellular senescence, and cell death. Under tolerable stress, cells activate adaptive antioxidant responses to promote survival, while chronic or severe stress leads to irreversible damage and cell death. This study suggests that targeting the PERK-mediated UPR pathway may present

a novel therapeutic strategy for overcoming senescence-induced treatment resistance in colon cancer. However, a limitation of this study is the inability to perform RT-*q*PCR at higher palmitic acid concentrations due to toxicity, restricting the analysis to adaptive senescence mechanisms observed at lower concentrations.

Declaration of competing interest

The authors declare that they have no competing interests.

Appendix A. Supplementary data

Supplementary data for this article are provided in Supplementary Fig 1 and Supplementary Fig 2

Availability of data and materials

The original contributions of this study are detailed in the article, and further inquiries are available upon request.

Acknowledgement

The authors acknowledge the Department of Biochemistry, Amala Cancer Research Centre, Thrissur, Kerala, for providing all the facilities to conduct the research work. The first author is thankful to the Council of Scientific and Industrial Research (CSIR), New Delhi for the financial support (No: 21/12/2014(ii)EU-V dt. 24/7/2015).

Credit authorship contribution statement

Soumy V V: Conceptualization, Data curation, Funding acquisition, Investigation, Methodology, Validation, Writing – original draft. Snijesh V P: methodology, Software, Data Curation, Binoy C F: supervision, investigation, validation. Achuthan C R: Formal analysis, investigation, resource, supervision and validation. Dr. Suraj K: Former analysis, resources, supervision, validation, review & editing. Babu T D: Conceptualization, formal analysis, investigation, methodology, project administration, resources, supervision, validation, writing – review & editing.

Funding

Council of Scientific and Industrial Research (CSIR), India

References

[1]. F. Huang, B. Sun, X. Wang, X. Jian, Q. Du, and J. Chen, "Dietary palmitic acid promotes tumor growth and epithelial-mesenchymal transformation in prostate cancer," 2021.

[2]. S. Fatima *et al.*, "High-fat diet feeding and palmitic acid increase CRC growth in β2AR-dependent manner," vol. 10, no. 10, p. 711, 2019.

[3]. L. Yang, G. Guan, L. Lei, J. Liu, L. Cao, and X. J. B. r. Wang, "Oxidative and endoplasmic reticulum stresses are involved in palmitic acid-induced H9c2 cell apoptosis," vol. 39, no. 5, p. BSR20190225, 2019.

[4]. C. Hetz, K. Zhang, and R. J. J. N. r. M. c. b. Kaufman, "Mechanisms, regulation and functions of the unfolded protein response," vol. 21, no. 8, pp. 421-438, 2020.

[5]. M.-Z. Wu *et al.*, "LncRNA GOLGA2P10 is induced by PERK/ATF4/CHOP signaling and protects tumor cells from ER stress-induced apoptosis by regulating Bcl-2 family members," vol. 11, no. 4, p. 276, 2020.

[6]. A. Tóth *et al.*, "Activation of PERK/eIF2α/ATF4/CHOP branch of endoplasmic reticulum stress response and cooperation between HIF-1α and ATF4 promotes Daprodustat-induced vascular calcification," vol. 15, p. 1399248, 2024.

[7]. R. Ernst, M. F. Renne, A. Jain, and A. J. C. S. H. P. i. B. von der Malsburg, "Endoplasmic reticulum membrane homeostasis and the unfolded protein response," p. a041400, 2024.

[8]. S. Bernales, F. R. Papa, and P. J. A. R. C. D. B. Walter, "Intracellular signaling by the unfolded protein response," vol. 22, no. 1, pp. 487-508, 2006.

[9]. W. Zhang *et al.*, "Endoplasmic reticulum stress—a key guardian in cancer," vol. 10, no. 1, p. 343, 2024.

[10]. B. Yang, S. Wang, Y. Yang, X. Li, F. Yu, and T. J. F. i. I. Wang, "Endoplasmic reticulum stress in breast cancer: a predictive model for prognosis and therapy selection," vol. 15, p. 1332942, 2024.

[11]. C. Panico *et al.*, "Single-cell RNA sequencing reveals metabolic stress-dependent activation of cardiac macrophages in a model of dyslipidemia-induced diastolic dysfunction," vol. 150, no. 19, pp. 1517-1532, 2024.

[12]. W. G. Glanzner *et al.*, "NRF2 attenuation aggravates detrimental consequences of metabolic stress on cultured porcine parthenote embryos," vol. 14, no. 1, p. 2973, 2024.

[13]. Y. Shi, B. Jiang, J. J. B. Zhao, and Pharmacotherapy, "Induction mechanisms of autophagy and endoplasmic reticulum stress in intestinal ischemia-reperfusion injury, inflammatory bowel disease, and colorectal cancer," vol. 170, p. 115984, 2024.

[14]. R. J. de Boer, J. v. L. de Jeude, and J. J. C. L. Heijmans, "ER stress and the unfolded protein response in gastrointestinal stem cells and carcinogenesis," p. 216678, 2024.

[15]. D. Li *et al.*, "Interactions between oxidative stress and senescence in cancer: mechanisms, therapeutic implications, and future perspectives," vol. 73, p. 103208, 2024.

[16]. R. Di Micco, V. Krizhanovsky, D. Baker, and F. J. N. r. M. c. b. d'Adda di Fagagna, "Cellular senescence in ageing: from mechanisms to therapeutic opportunities," vol. 22, no. 2, pp. 75-95, 2021.

[17]. M. Ketkar *et al.*, "Inhibition of PERK-mediated unfolded protein response acts as a switch for reversal of residual senescence and as senolytic therapy in glioblastoma," vol. 26, no. 11, pp. 2027-2043, 2024.

[18]. A. M. Burgos-Molina, T. Téllez Santana, M. Redondo, and M. J. J. I. J. o. M. S. Bravo Romero, "The Crucial Role of Inflammation and the Immune System in Colorectal Cancer Carcinogenesis: A Comprehensive Perspective," vol. 25, no. 11, p. 6188, 2024.

[19]. A. L. Theiss and C. S. J. G. Williams, "Burn the fat: colon cancer tumors are skilled at lipid storage during obesity," 2024.

[20]. M. Zafaryab, K. U. Fakhri, M. A. Khan, K. Hajela, and M. M. A. J. I. J. L. S. R. Rizvi, "In vitro assessment of cytotoxic and apoptotic potential of palmitic acid for breast cancer treatment," vol. 7, no. 1, pp. 166-174, 2019.

[21]. G. Sharma, A. Parihar, P. Parihar, M. S. J. J. o. B. Parihar, and M. Toxicology, "Downregulation of sirtuin 3 by palmitic acid increases the oxidative stress, impairment of mitochondrial function, and apoptosis in liver cells," vol. 33, no. 8, p. e22337, 2019.

[22]. Y. Chen *et al.*, "PNPLA3 148M/M Is More Susceptible to Palmitic Acid-Induced Endoplasmic Reticulum Stress-Associated Apoptosis in HepG2 Cells," vol. 2023, no. 1, p. 2872408, 2023.

[23]. N. Brix, D. Samaga, R. Hennel, K. Gehr, H. Zitzelsberger, and K. Lauber, "The clonogenic assay: robustness of plating efficiency-based analysis is strongly compromised by cellular cooperation," *Radiation Oncology,* vol. 15, no. 1, p. 248, 2020/10/29 2020.

[24]. X. Hu *et al.*, "Effects of saturated palmitic acid and omega-3 polyunsaturated fatty acids on Sertoli cell apoptosis," (in eng), *Syst Biol Reprod Med,* vol. 64, no. 5, pp. 368-380, Oct 2018.

[25]. O. H. Lowry, N. J. Rosebrough, A. L. Farr, and R. J. Randall, "Protein measurement with the Folin phenol reagent," (in eng), *J Biol Chem,* vol. 193, no. 1, pp. 265-75, Nov 1951.

[26]. R. F. Beers, Jr. and I. W. Sizer, "A spectrophotometric method for measuring the breakdown of hydrogen peroxide by catalase," (in eng), *J Biol Chem,* vol. 195, no. 1, pp. 133-40, Mar 1952.

[27]. J. M. McCord and I. Fridovich, "Superoxide dismutase. An enzymic function for erythrocuprein (hemocuprein)," (in eng), *J Biol Chem,* vol. 244, no. 22, pp. 6049-55, Nov 25 1969.

[28]. W. H. Habig, M. J. Pabst, and W. B. J. J. o. b. C. Jakoby, "Glutathione S-transferases: the first enzymatic step in mercapturic acid formation," vol. 249, no. 22, pp. 7130-7139, 1974.

[29]. P. C. Simons and D. L. J. A. B. Vander Jagt, "Purification of glutathione S-transferases from human liver by glutathione-affinity chromatography," vol. 82, no. 2, pp. 334-341, 1977.

[30]. R. D. Mavis and E. J. J. o. B. C. Stellwagen, "Purification and subunit structure of glutathione reductase from bakers' yeast," vol. 243, no. 4, pp. 809-814, 1968.

[31]. E. Racker, "[127] Glutathione reductase1 (liver and yeast)," 1955.

[32]. I. Rahman, A. Kode, and S. K. J. N. p. Biswas, "Assay for quantitative determination of glutathione and glutathione disulfide levels using enzymatic recycling method," vol. 1, no. 6, pp. 3159-3165, 2006.

[33]. D. E. Paglia, W. N. J. T. J. o. l. Valentine, and c. medicine, "Studies on the quantitative and qualitative characterization of erythrocyte glutathione peroxidase," vol. 70, no. 1, pp. 158-169, 1967.

[34]. H. Ohkawa, N. Ohishi, and K. J. A. b. Yagi, "Assay for lipid peroxides in animal tissues by thiobarbituric acid reaction," vol. 95, no. 2, pp. 351-358, 1979.

[35]. D. R. Beriault and G. H. J. B. e. B. A.-M. C. R. Werstuck, "Detection and quantification of endoplasmic reticulum stress in living cells using the fluorescent compound, Thioflavin T," vol. 1833, no. 10, pp. 2293-2301, 2013.

[36]. K. J. Livak and T. D. J. m. Schmittgen, "Analysis of relative gene expression data using real-time quantitative PCR and the 2− ΔΔCT method," vol. 25, no. 4, pp. 402-408, 2001.

[37]. B. Xu *et al.*, "Inositol hexaphosphate enhances chemotherapy by reversing senescence induced by persistently activated PERK and diphthamide modification of eEF2," vol. 582, p. 216591, 2024.

[38]. S. Andrews, "FastQC: a quality control tool for high throughput sequence data. 2010," ed, 2017.

[39]. F. Krueger, "TrimGalore: A wrapper tool around Cutadapt and FastQC to consistently apply quality and adapter trimming to FastQ files. Babraham Bioinformatics," ed, 2015.

[40]. A. Dobin *et al.*, "STAR: ultrafast universal RNA-seq aligner," vol. 29, no. 1, pp. 15-21, 2013.

[41]. Y. Liao, G. K. Smyth, and W. J. B. Shi, "featureCounts: an efficient general purpose program for assigning sequence reads to genomic features," vol. 30, no. 7, pp. 923-930, 2014.

[42]. M. I. Love, W. Huber, and S. J. G. b. Anders, "Moderated estimation of fold change and dispersion for RNA-seq data with DESeq2," vol. 15, pp. 1-21, 2014.

[43]. V. P. Nimbalkar *et al.*, "Premenopausal women with breast cancer in the early post-partum period show molecular profiles of invasion and are associated with poor prognosis," vol. 200, no. 1, pp. 139-149, 2023.

[44]. L. Fusée *et al.*, "The p53 endoplasmic reticulum stress-response pathway evolved in humans but not in mice via PERK-regulated p53 mRNA structures," *Cell Death & Differentiation,* vol. 30, no. 4, pp. 1072-1081, 2023/04/01 2023.

[45]. G. Alasiri *et al.*, "Reciprocal regulation between GCN2 (eIF2AK4) and PERK (eIF2AK3) through the JNK-FOXO3 axis to modulate cancer drug resistance and clonal survival," *Molecular and Cellular Endocrinology,* vol. 515, p. 110932, 2020/09/15/ 2020.

[46]. L. D. Ly *et al.*, "Oxidative stress and calcium dysregulation by palmitate in type 2 diabetes," (in eng), *Exp Mol Med,* vol. 49, no. 2, p. e291, Feb 3 2017.

[47]. G. Carta, E. Murru, S. Banni, and C. Manca, "Palmitic Acid: Physiological Role, Metabolism and Nutritional Implications," (in eng), *Front Physiol*, vol. 8, p. 902, 2017.

[48]. S. Beloribi-Djefaflia, S. Vasseur, and F. J. O. Guillaumond, "Lipid metabolic reprogramming in cancer cells," vol. 5, no. 1, pp. e189-e189, 2016.

[49]. C. Schiliro and B. L. J. C. Firestein, "Mechanisms of metabolic reprogramming in cancer cells supporting enhanced growth and proliferation," vol. 10, no. 5, p. 1056, 2021.

[50]. M. Correia de Sousa, E. Delangre, M. Türkal, M. Foti, and M. J. I. J. o. M. S. Gjorgjieva, "Endoplasmic reticulum stress in renal cell carcinoma," vol. 24, no. 5, p. 4914, 2023.

[51]. J. Mikuła-Pietrasik, A. Niklas, P. Uruski, A. Tykarski, K. J. C. Książek, and M. L. Sciences, "Mechanisms and significance of therapy-induced and spontaneous senescence of cancer cells," vol. 77, pp. 213-229, 2020.

[52]. S. Lee and C. A. J. N. c. b. Schmitt, "The dynamic nature of senescence in cancer," vol. 21, no. 1, pp. 94-101, 2019.

[53]. S. Chen *et al.*, "New insights into the role of mitochondrial dynamics in oxidative stress-induced diseases," vol. 178, p. 117084, 2024.

[54]. L. V. Bel'skaya and E. I. J. C. I. i. M. B. Dyachenko, "Oxidative Stress in Breast Cancer: A Biochemical Map of Reactive Oxygen Species Production," vol. 46, no. 5, pp. 4646-4687, 2024.

[55]. X. Chen *et al.*, "Palmitic acid induces lipid droplet accumulation and senescence in nucleus pulposus cells via ER-stress pathway," vol. 7, no. 1, p. 539, 2024.

[56]. J. M. Matés, J. A. Segura, F. J. Alonso, and J. J. A. o. t. Márquez, "Intracellular redox status and oxidative stress: implications for cell proliferation, apoptosis, and carcinogenesis," vol. 82, pp. 273-299, 2008.

[57]. M. R. Chaudhary *et al.*, "Aging, oxidative stress and degenerative diseases: mechanisms, complications and emerging therapeutic strategies," vol. 24, no. 5, pp. 609-662, 2023.

[58]. S. X. Mthembu *et al.*, "Low levels and partial exposure to palmitic acid improves mitochondrial function and the oxidative status of cultured cardiomyoblasts," vol. 12, pp. 234-243, 2024.

[59]. B. Vidrio-Huerta, T. Plötz, and S. J. J. o. M. E. Lortz, "Oxidative and ER stress by elevated insulin biosynthesis and palmitic acid in insulin-producing cells," vol. 72, no. 2, 2024.

[60]. M. D. Yener, T. Çolak, Ö. D. Özsoy, and F. C. J. J. o. I. F. o. M. Eraldemir, "ALTERATIONS IN CATALASE, SUPEROXIDE DISMUTASE, GLUTATHIONE PEROXIDASE AND MALONDIALDEHYDE LEVELS IN SERUM AND LIVER TISSUE UNDER STRESS CONDITIONS," vol. 87, no. 2, pp. 145-152, 2024.

[61]. A. Alnahdi, A. John, and H. J. N. Raza, "Augmentation of glucotoxicity, oxidative stress, apoptosis and mitochondrial dysfunction in HepG2 cells by palmitic acid," vol. 11, no. 9, p. 1979, 2019.

[62]. E.-J. Park, A. Y. Lee, S. Park, J.-H. Kim, M.-H. J. F. Cho, and C. Toxicology, "Multiple pathways are involved in palmitic acid-induced toxicity," vol. 67, pp. 26-34, 2014.

[63]. Q. Zhang *et al.*, "Reprogramming of palmitic acid induced by dephosphorylation of ACOX1 promotes β-catenin palmitoylation to drive colorectal cancer progression," vol. 9, no. 1, p. 26, 2023.

[64]. X. Zhang *et al.*, "Palmitic acid promotes lung metastasis of melanomas via the TLR4/TRIF-Peli1-pNF-κB pathway," vol. 12, no. 11, p. 1132, 2022.

[65]. G. Porter, "Dissecting the role of endoplasmic reticulum stress in cancer progression," UNSW Sydney, 2024.

[66]. A. Griffiths *et al.*, "ATF4-mediated CD36 upregulation contributes to palmitate-induced lipotoxicity in hepatocytes," vol. 324, no. 5, pp. G341-G353, 2023.

[67]. H. Cho, M. Wu, L. Zhang, R. Thompson, A. Nath, and C. Chan, "Signaling dynamics of palmitate-induced ER stress responses mediated by ATF4 in HepG2 cells," *BMC Systems Biology*, vol. 7, no. 1, p. 9, 2013/01/22 2013.

[68]. Y. Wang *et al.*, "The unfolded protein response induces the angiogenic switch in human tumor cells through the PERK/ATF4 pathway," vol. 72, no. 20, pp. 5396-5406, 2012.

[69]. A. Nagelkerke *et al.*, "Hypoxia stimulates migration of breast cancer cells via the PERK/ATF4/LAMP3-arm of the unfolded protein response," vol. 15, pp. 1-13, 2013.

[70]. L. Carciero *et al.*, "The interplay of extracellular vesicles in the pathogenesis of metabolic impairment and type 2 diabetes," p. 111837, 2024.

[71]. Y. Fang *et al.*, "Inhibition of SLC40A1 represses osteoblast formation via inducing iron accumulation and activating the PERK/ATF4/CHOP pathway mediated oxidative stress," vol. 29, no. 1, p. 2428147, 2024.

[72]. L. Liu *et al.*, "Qing Hua Chang Yin ameliorates chronic colitis in mice by inhibiting PERK–ATF4–CHOP pathway of ER stress and the NF-κB signalling pathway," vol. 62, no. 1, pp. 607-620, 2024.

[73]. Y. Zhang, R. Xue, Z. Zhang, X. Yang, H. J. L. i. h. Shi, and disease, "Palmitic and linoleic acids induce ER stress and apoptosis in hepatoma cells," vol. 11, pp. 1-8, 2012.

[74]. C. Sarcinelli *et al.*, "ATF4-dependent NRF2 transcriptional regulation promotes antioxidant protection during endoplasmic reticulum stress," vol. 12, no. 3, p. 569, 2020.

[75]. S. B. Cullinan, J. A. J. T. i. j. o. b. Diehl, and c. biology, "Coordination of ER and oxidative stress signaling: the PERK/Nrf2 signaling pathway," vol. 38, no. 3, pp. 317-332, 2006.

[76]. S. B. Cullinan *et al.*, "Nrf2 is a direct PERK substrate and effector of PERK-dependent cell survival," vol. 23, no. 20, pp. 7198-7209, 2003.

[77]. J. Wang *et al.*, "Up-regulation of PERK/Nrf2/HO-1 axis protects myocardial tissues of mice from damage triggered by ischemia-reperfusion through ameliorating endoplasmic reticulum stress," vol. 10, no. 3, p. 500, 2020.

[78]. J. H. Lee and J. Lee, "Endoplasmic Reticulum (ER) Stress and Its Role in Pancreatic β-Cell Dysfunction and Senescence in Type 2 Diabetes," (in eng), *Int J Mol Sci,* vol. 23, no. 9, Apr 27 2022.

[79]. Z. Z. Ei *et al.*, "GRP78/BiP determines senescence evasion cell fate after cisplatin-based chemotherapy," *Scientific Reports,* vol. 11, no. 1, p. 22448, 2021/11/17 2021.

[80]. D. R. Fels, C. J. C. b. Koumenis, and therapy, "The PERK/eIF2α/ATF4 module of the UPR in hypoxia resistance and tumor growth," vol. 5, no. 7, pp. 723-728, 2006.

[81]. S. Courtois-Cox *et al.*, "A negative feedback signaling network underlies oncogene-induced senescence," vol. 10, no. 6, pp. 459-472, 2006.

[82]. J. J. A. r. o. p. Campisi, "Aging, cellular senescence, and cancer," vol. 75, no. 1, pp. 685-705, 2013.

[83]. X. W. Wang *et al.*, "GADD45 induction of a G2/M cell cycle checkpoint," vol. 96, no. 7, pp. 3706-3711, 1999.

[84]. X. Palomer, J. M. Salvador, C. Griñán-Ferré, E. Barroso, M. Pallàs, and M. J. M. R. R. Vázquez-Carrera, "GADD45A: With or without You," vol. 44, no. 4, pp. 1375-1403, 2024.

[85]. N. Wechter *et al.*, "Single-cell transcriptomic analysis uncovers diverse and dynamic senescent cell populations," (in eng), *Aging (Albany NY),* vol. 15, no. 8, pp. 2824-2851, Apr 19 2023.

[86]. M. J. P. B. Rusin, "The p53 protein–not only the guardian of the genome," vol. 70, no. 1, pp. 71-87, 2024.

[87]. S. Martello *et al.*, "Developing an RNA Signature for Radiation Injury Using a Human Liver-on-a-Chip Model," vol. 202, no. 3, pp. 489-502, 2024.